

## Microstructure, properties investigations and methodology of the state evaluation of T23 (2.25Cr-0.3Mo-1.6W-V-Nb) steel in boilers application

J. Dobrzański <sup>a,\*</sup>, A. Zieliński <sup>a</sup>, M. Sroka <sup>b</sup>

<sup>a</sup> Institute for Ferrous Metallurgy, ul. K. Miarki 12/14, 44-100 Gliwice, Poland

<sup>b</sup> Division of, Materials Processing Technologies, Management and Computer Techniques in Materials Science, Institute of Engineering Materials and Biomaterials, Silesian University of Technology, ul. Konarskiego 18a, 44-100 Gliwice, Poland

\* Corresponding author: E-mail address: jdobrzanski@imz.gliwice.pl

Received 19.02.2007; published in revised form 01.02.2009

### Materials

#### ABSTRACT

**Purpose:** The purpose of the paper is to work out the classification of the structure's changes and the development of precipitation processes and the internal damages related to the exhaust degree of material working in creep conditions to use in the materials diagnostics.

**Design/methodology/approach:** Examination results were made on materials in initial state, after long-lasting annealing and after creep trials. Investigations of the structure were made by the use TEM, and morphology of internal damages resulting from creep were made by the use of scanning electron microscope.

**Findings:** The paper presents investigation results in the area of the changes of mechanical properties and structure of the T23 steel resulting from the long term impact of temperature and load in conditions corresponding to the service ones. The influence on mechanical properties and structure after long-lasting temperature and load exposition was estimated. Schemes of structure changes and inner failures after exposition in creep condition were worked out.

**Practical implications:** The worked out methodology of evaluation of the material's state after exploitation in creep conditions can be use in the material's diagnostics of element working in power industry.

**Originality/value:** Classification of the structure changes and development of precipitation processes and internal damages as a result of creep.

**Keywords:** Steel T23; Structure; Creep; Image analysis

**Reference to this paper should be given in the following way:**

J. Dobrzański, A. Zieliński, M. Sroka, Microstructure, properties investigations and methodology of the state evaluation of T23 (2.25Cr-0.3Mo-1.6W-V-Nb) steel in boilers application, Journal of Achievements in Materials and Manufacturing Engineering 32/2 (2009) 142-153.

## 1. Introduction

Continuous progress in the power generation industry calls for creep resistant materials, and especially for steel for manufacturing the pressure boiler elements in service at elevated temperature (chambers, pipelines, coil pipes). Increasing quality requirements, increasing the service parameters (like temperature and pressure), improvement of efficiency and reliability, as well as the economic issue impose the intensified activity in the area of modernization, diagnostics, and extension of life of the power systems and their elements. Extension of the safe service period above the design period assumed at their design stage is reduced to determining the so called residual life. It is defined as the difference between the time to damage and the real service time.

Computer applications, simulation programs or expert systems are used more and more often as the computer assistance tools to make the engineering tasks easier and to improve their efficiency [1, 5-7, 11]. Neural networks, apart from the genetic algorithms are the tools with which one can, among others, not only identify the image but also merge all preceding initial digital image processing stages. The advantages of neural networks decide about their more and more widespread use in carrying out many tasks of an engineering nature, also as applications assisting humans in taking difficult and very often very complex decisions [8, 9, 12, 16, 17].

Employment of the new generation steels from the low-alloy steel group with the ferritic-bainitic structure of the 2.5 Cr-Mo type with vanadium, tungsten, and micro-additions for elements of the power systems of the supercritical power boilers forces carrying out periodic diagnostic examinations and carrying out evaluation of the condition and the life exhaustion extent of the elements' material and determining their usefulness for further service [4]. Data describing material behaviour in service subjected to the simultaneous effect of temperature and applied stress are indispensable to carry out such investigations.

The paper presents investigation results in the area of the changes of mechanical properties and structure of the T23 steel resulting from the long term impact of temperature and load in conditions corresponding to the service ones. Moreover, it presents the main elements of the computer method for the automatic classification of the damage extent of the investigated steel in creep service, assisting evaluation of its state. The paper does not exhaust the discussed subject and is only the first stage of the solving the problem pertaining to material diagnostics of the power systems elements operating in creep service and made from the investigated T23 steel.

## 2. Material and research methodology

Investigations were made of the low-alloy steel with the ferritic-bainitic of the T23 (2.25Cr-0.3Mo-1.6W-V-Nb) grade in the shape of the thick-wall seamless tube. The investigated tube from the T23 steel was in the normalized and tempered state, according to the technical requirements for these products. The chemical composition of the investigated tube material is presented in Table 1. Moreover, requirements are also specified in the table for the investigated material grade in this regard [3, 5, 18-20].

## 3. Experimental

The following investigations were carried out within the project framework:

- temperature effect on changes of the mechanical properties,
- temperature and long-time annealing effect on structure, hardness, impact strength, and fracture nature,
- temperature, time, and stress effect on precipitation processes and development of the internal defects,
- a computer based method of assisting analysis of the structure changes and automatic classification of the extent of life exhaustion extent.

### 3.1. Mechanical properties at elevated temperature

Results of the mechanical properties tests at room temperature and at elevated temperature of the investigated tube from the low-alloy T23 steel after normalizing and tempering are shown in the graphical form in Figure 1.

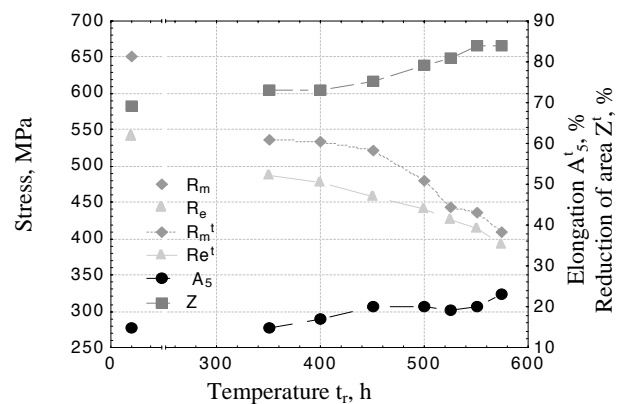


Fig. 1. Mechanical properties at room temperature and at elevated temperature of the investigated tube from the low-alloy T23 steel in the normalized and tempered states [3]

### 3.2. Changes of hardness and impact strength after long-time annealing

Impact strength and hardness tests were carried on test pieces after annealing at the temperatures of  $T_a = 550$  and  $600^\circ\text{C}$  with the duration of up to 3000 hours. Long time annealing tests are carried out, whose expected completion time will be 5000 and 10000 hours. However, these tests were not completed yet. The obtained impact strength tests results in the form of the relationship  $KCV = f(t_a)$  for  $T_a = 550$  and  $600^\circ\text{C}$ , where  $t_a$  – annealing time, a  $T_a$  – test temperature, are shown in Figure 2a and the HV10 hardness test results in the form of the relationship  $HV10 = f(t_a)$  for  $T_a = 550$  and  $600^\circ\text{C}$  are shown in Figure 2b.

Table 1.

## Chemical composition of the steel

Type of steel heat	Concentration of elements [wt.%]														Notes
	C	Mn	Si	P	S	Cr	Ni	Mo	V	W	Nb	B	Al	N	
T23 pipe $\phi$ 273x40	0.04-	0.10	max.	max.	max.	1.90-	-	0.05-	0.20-	1.45-	0.02-	0.0005-	max.	max.	ASTM A213/A2 13M-99A
	0.10	-	0.50	0.03	0.01	2.60	-	0.30	0.30	1.75	0.08	0.006	0.03	0.03	
	0.058	0.46	0.20	0.014	0.001	2.18	0.14	0.08	0.25	1.54	0.05	0.0023	0.001	0.0023	

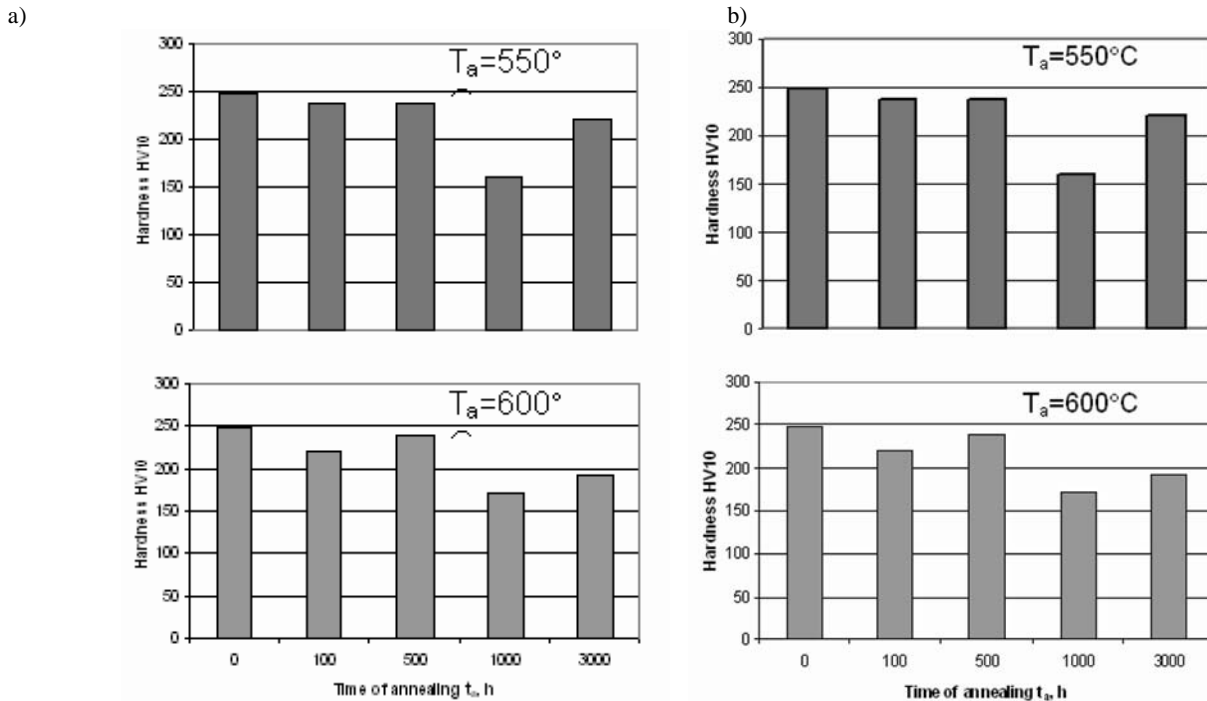
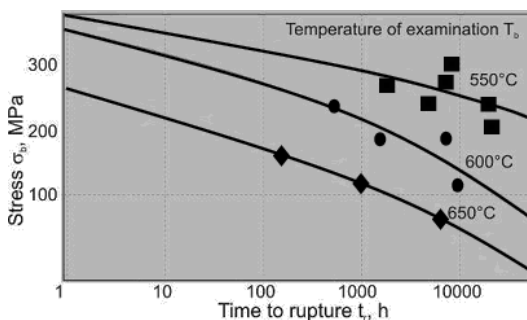


Fig. 2. Tempering time and temperature of the T23 steel effect in its normalized and tempered states on: a) impact strength b) hardness

### 3.3. Creep strength

Creep test results up to rupture in the form of the relationship  $\lg \sigma_b = f(\lg t_r)$  at  $T_b = \text{const}$ ; where  $\sigma_b$  – test stress,  $t_r$  – time to rupture,  $T_b$  – test temperature, is presented for the T23 steel at temperatures  $T_b = 550, 600$  and  $650^\circ\text{C}$  in Figure 3.

Fig. 3. Creep tests results up to rupture of the T23 steel in the form of the relationship  $\lg \sigma_b = f(\lg t_r)$  at  $T_b = \text{const}$ . for  $T_b = 550; 600, 650^\circ\text{C}$ 

### 3.4. Microstructure and failure examinations. Development of precipitation and internal damage processes

Results of structure examinations and effect of the annealing time of the T23 steel on nature of the fractographic images of the obtained fractures in the impact strength test pieces observed on the scanning electron microscope after annealing for 1000 and 3000 hours at the temperatures of  $T_a = 550^\circ\text{C}$  and  $T_a = 600^\circ\text{C}$  compared to the initial state structure image compared to the KCV impact strength results for the investigated T23 steel are shown in Figures 4 and 5 respectively.

Investigations of the effect of the temperature, time, and stress on structure changes, development of the precipitation processes, and development of the internal defects were carried out on the test pieces after the creep tests, according to the test results shown in Figure 2.

Changes occurring in the structure image of the T23 steel observed on the metallographic micro-sections on the scanning electron microscope depending on the test temperature  $T_b$  and stress  $\sigma_b$  with the creep resistance curves in the form of the relationship  $\lg \sigma_b = f(\lg t_r)$  at  $T_b = \text{const}$  are presented in Figure 6.

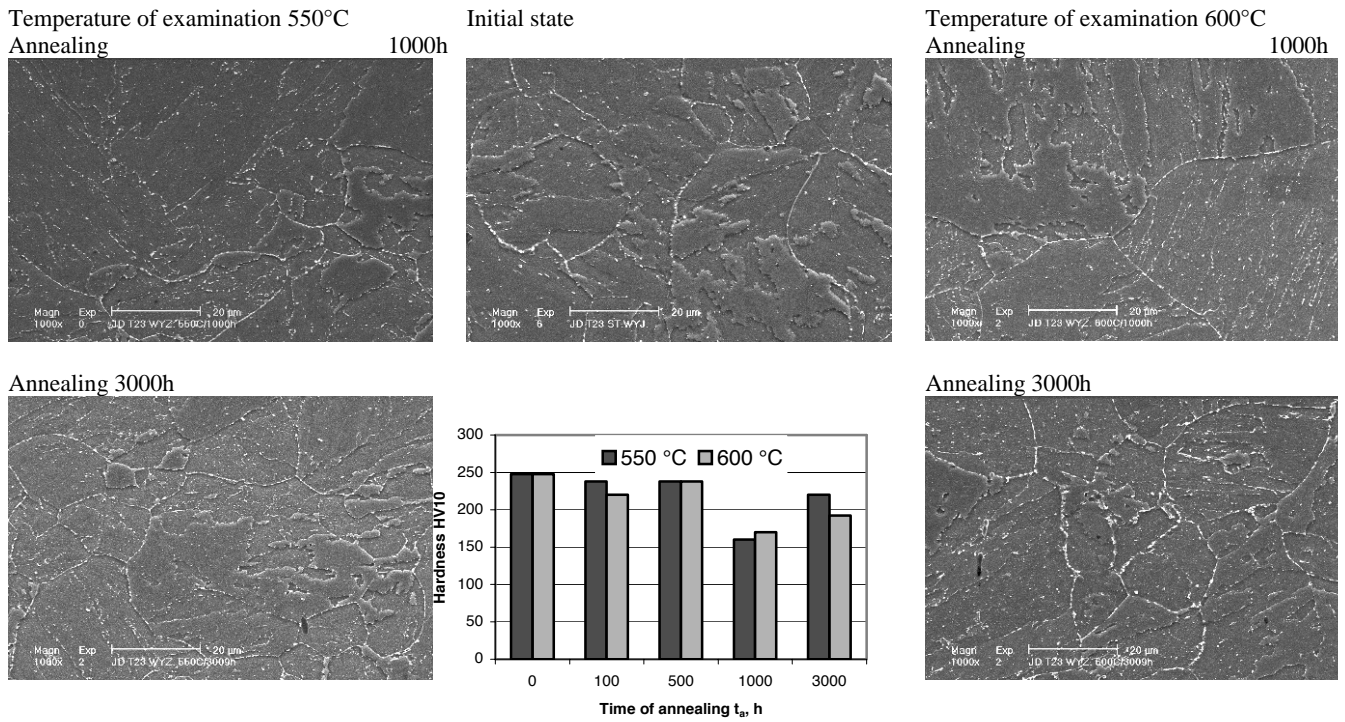


Fig. 4. Effect of the long term annealing time at the test temperatures of  $T_a = 550^\circ\text{C}$  and  $600^\circ\text{C}$  on changes of the structure of the T23 steel in its normalized and tempered states observed on SEM

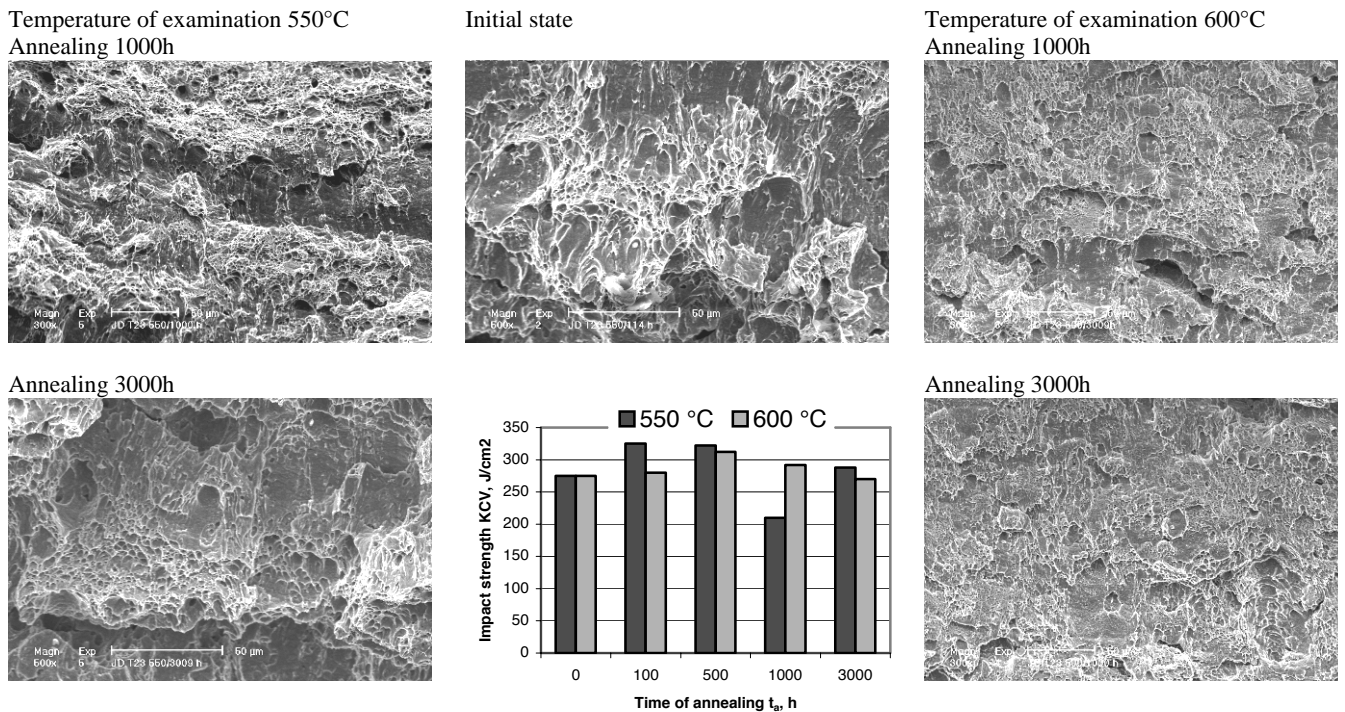


Fig 5. Effect of the long term annealing time at the test temperatures of  $T_b = 550^\circ\text{C}$  and  $600^\circ\text{C}$  on changes of the fractures fractography images of the impact strength test pieces of the T23 steel in its normalized and tempered states observed on SEM

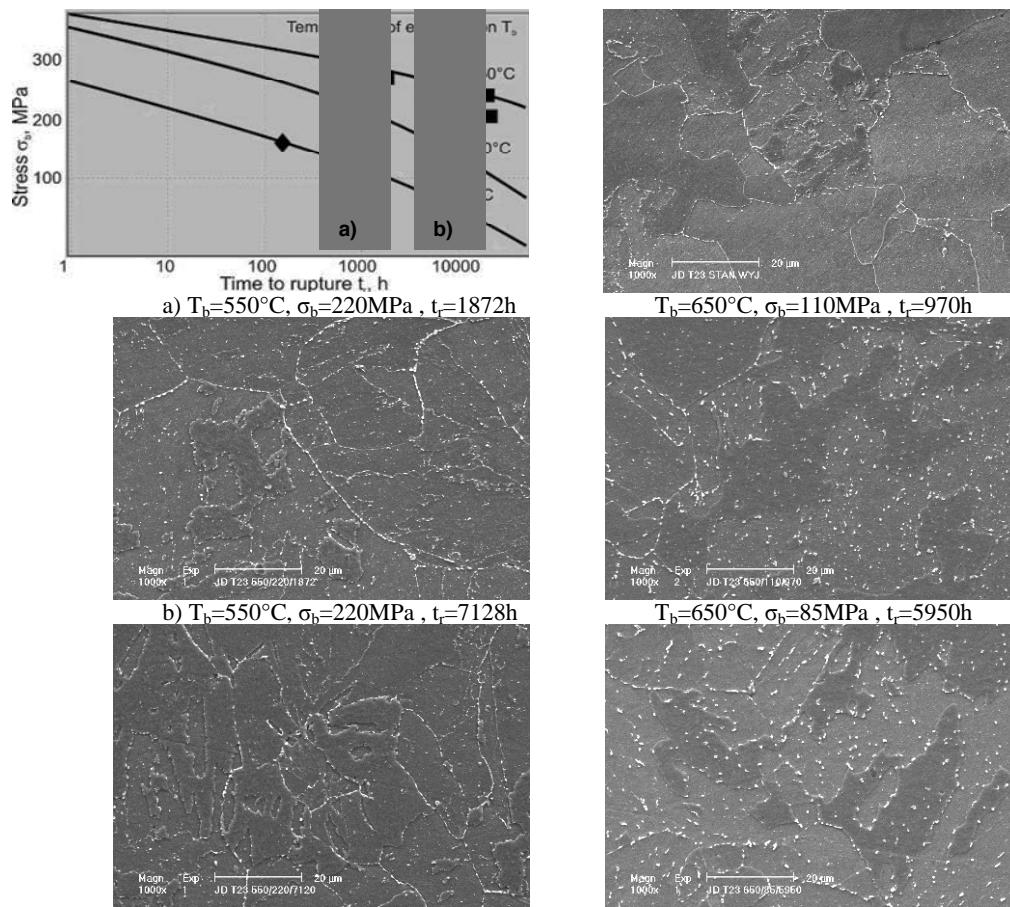


Fig. 6. Changes occurring in the T23 structure image due to creep; etched micro-section - scanning electron microscope

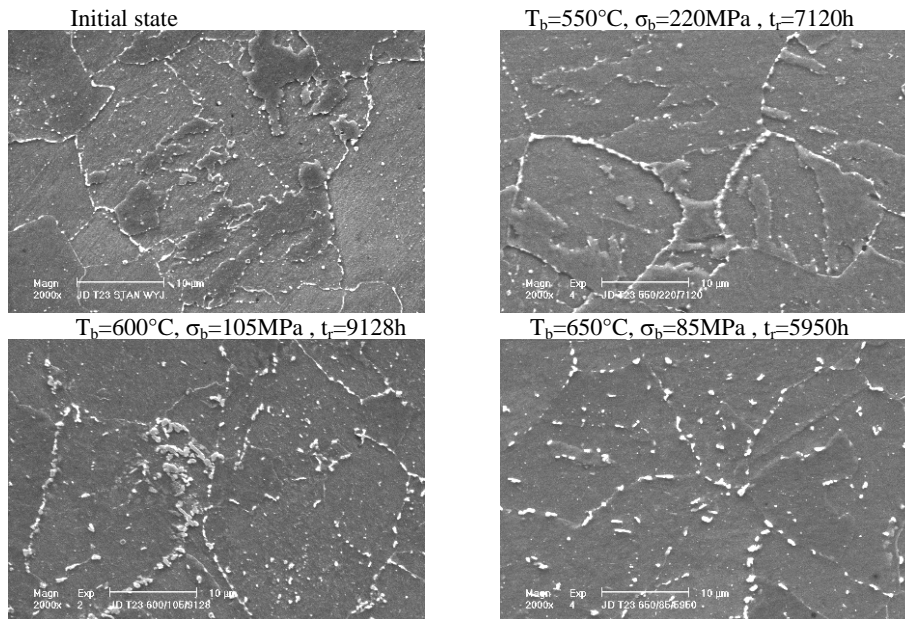


Fig. 7. Changes in the structure image of the T23 steel depending on the test temperature  $T_b$  for the time to rupture  $t_r$  in the creep test - scanning electron microscope (SEM)

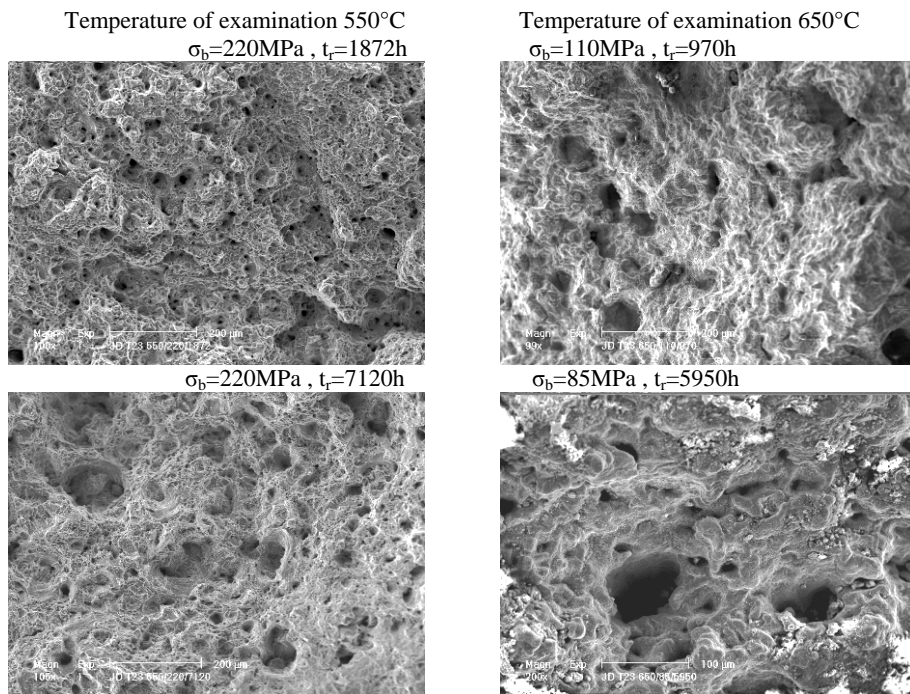


Fig. 8. Fractographic images of the test pieces fractures after creep to rupture of the T23 steel depending on the test temperature  $T_b$ , test stress  $\sigma_b$ , and time to rupture  $t_r$ ; fracture - scanning electron microscope (SEM)

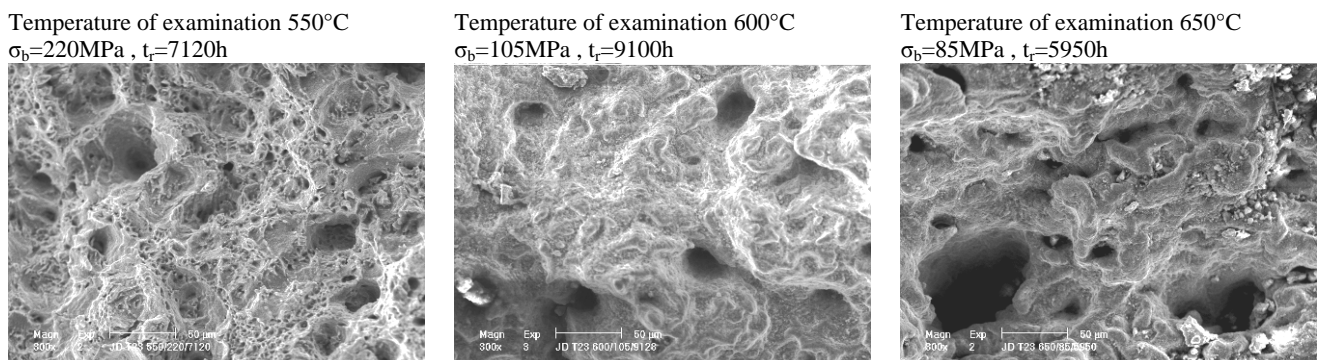


Fig. 9. Fractographic images of the test pieces fractures after creep to rupture of the T23 steel depending on the test temperature  $T_b$ , with the similar time to rupture  $t_r$ ; fracture - scanning electron microscope (SEM)

In Figure 7, however, structure changes of this steel are shown, depending on the test temperature  $T_b$  for the close time periods to break  $t_r$  in the creep test.

Analogously with the creep resistance curves in the background, the fractographic images of the test pieces fractures after creep to break are shown, obtained on the scanning electron microscope, in Figure 8 - depending on the test temperature  $T_b$  and stress  $\sigma_b$ , and in Figure 9 - depending on the test temperature  $T_b$  and with the similar time to break  $t_r$ .

Investigation of the precipitation processes development was carried out on thin foils collected from the T23 steel test pieces after long term annealing and creep. Microstructure was observed in the transmission electron microscope at magnifications from 6000 to 80000x. Test results after annealing for 1000 and 3000

hours at the temperature of  $T_b = 550^\circ\text{C}$  and  $600^\circ\text{C}$  are shown in Figures 10 - 13 respectively. The microstructure after creep for more than 10000 hours at the temperature of  $550^\circ\text{C}$  is shown in Figure 14.

Identification of the precipitations with the electron diffraction failed, as the observed particles were too bulky to give the diffraction pattern. Therefore, analysis of the precipitations was carried out in the discussion of the investigation results only based on the known morphological features of the particular precipitation types. Figure 15 shows investigation results of the internal damage processes developed in the creep process and observed on the scanning electron microscope on the microsections.

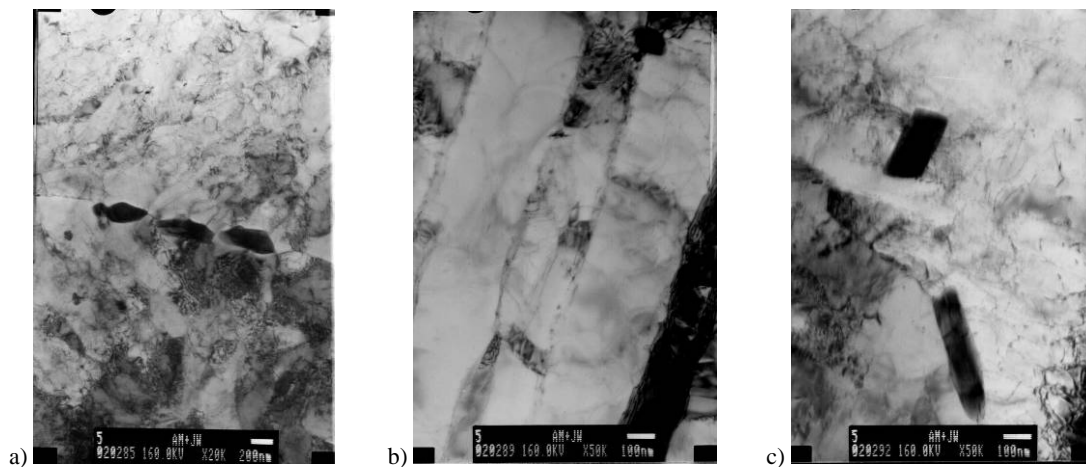


Fig. 10. Microstructure of the T23 steel after annealing for 1000h at the test temperature of  $T_b = 550^\circ\text{C}$ ; thin foil - transmission electron microscope (TEM), magnifications: a) 10 000x, b) 20 000x, c) 50 000x

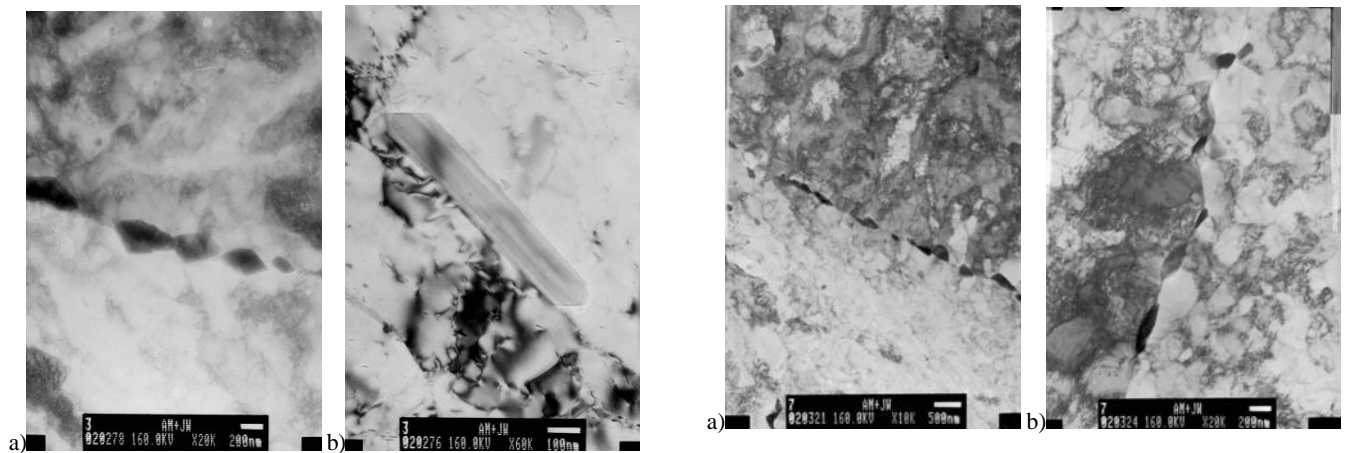


Fig. 11. Microstructure of the T23 steel after annealing for 3000h at the test temperature of  $T_b = 550^\circ\text{C}$ ; thin foil - transmission electron microscope (TEM), magnifications: a, b) 50 000x

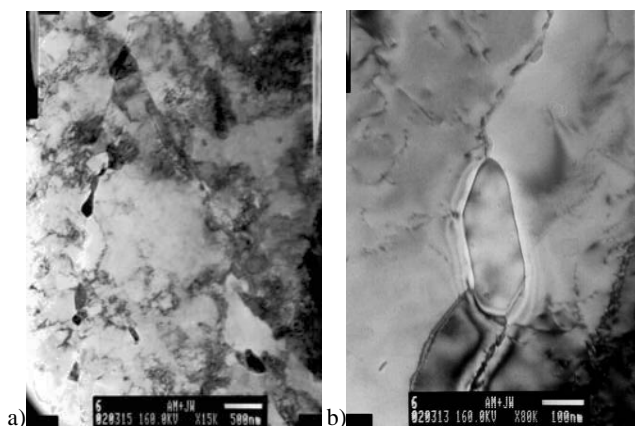


Fig. 12. Microstructure of the T23 steel after annealing for 1000h at the test temperature of  $T_b = 600^\circ\text{C}$ ; thin foil - transmission electron microscope (TEM), magnifications: a) 15 000x, b) 80 000x

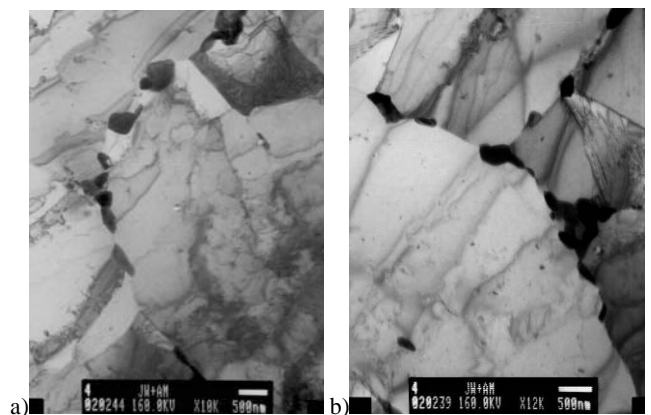


Fig. 13. Microstructure of the T23 steel after annealing at the test temperature of  $T_b = 600^\circ\text{C}$  for 3000h; thin foil - transmission electron microscope (TEM), magnifications: a) 10 000x, b) 15 000x

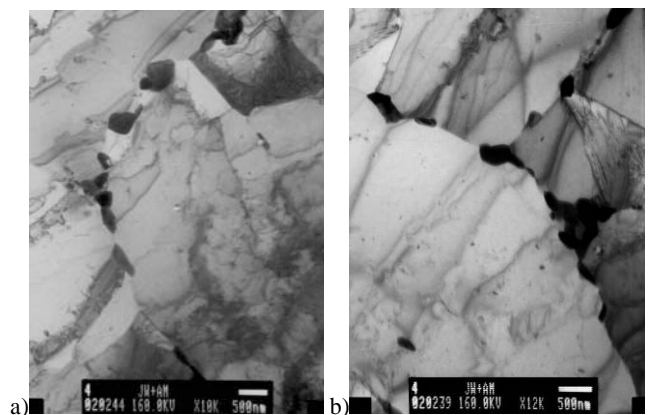
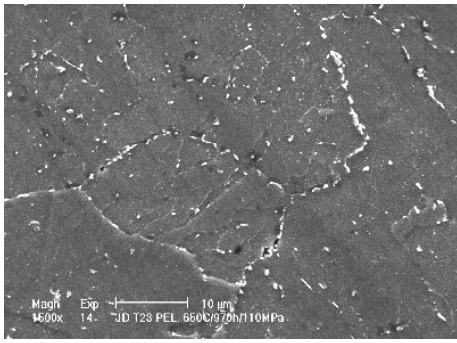
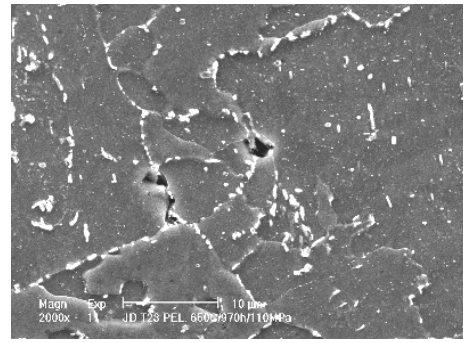


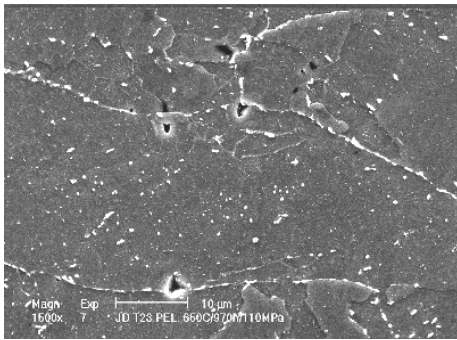
Figure 14. Microstructure of the T23 steel after creep test at the test temperature of  $T_b = 550^\circ\text{C}$  at the stress of  $\sigma_b = 110 \text{ MPa}$  and time to break  $t_r = 10\,400 \text{ h}$ ; thin foil - transmission electron microscope (TEM), magnifications: a) 10 000x, b) 20 000x



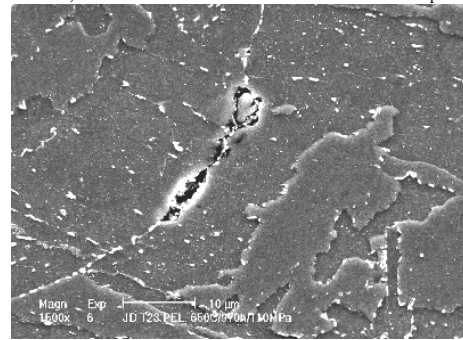
Single voids unevenly distributed (CLASS A/1; LIFE EXHAUSTION EXTENT)



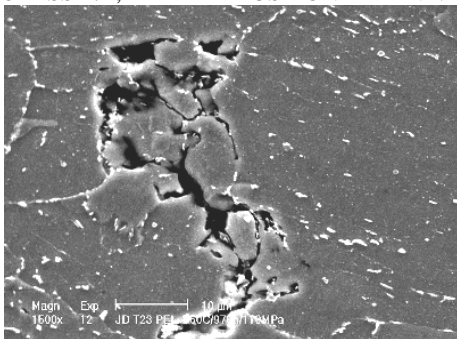
Single voids irregularly distributed on grain boundaries or sub-grains in the area of bainite (CLASS A/2; LIFE EXHAUSTION EXTENT:  $t/t_r \sim 0.5-0.8$ )



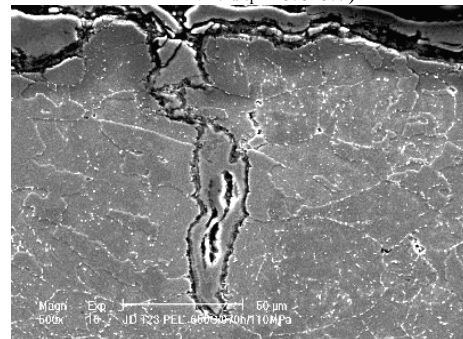
Voids oriented on grain boundaries or sub-grains in the area of bainite (CLASS B/1; LIFE EXHAUSTION EXTENT:  $t/t_r \sim 0.6$ )



Coalescence of the voids (CLASS B/3; LIFE EXHAUSTION EXTENT:  $t/t_r \sim 0.6-0.7$ )



Intercrystalline crevices encompassing a single grain (CLASS C/1; LIFE EXHAUSTION EXTENT:  $t/t_r \sim (0.7-0.8)$ )



Development of macro-cracks (CLASS D; LIFE EXHAUSTION EXTENT:  $t/t_r \sim 0.8-1.0$ )

Fig. 15. Consecutive stages of development of the internal defects and their relevant life exhaustion extent  $t/t_r$  in the low-alloy T23 steel with the ferritic-bainitic structure after long time service (classification according to Figure 17). Classification of the material state is given in parentheses

### 3.5. Methodology for automatic classification of the extent of life exhaustion extent

The computer assisted method was developed for automatic classification of the life exhaustion extent for the examined material. To standardize the analysed images they were saved in the bit map format with 256 grades of grey. Filtration was used during the initial processing. Adaptation filter form was selected

as a result of the experimental verification, whose task is to sharpen the edges and simultaneously to average areas outside these edges. The filter has a two-stage operation and its characteristics changes depending on the analysed area. The first stage consists in determining for each point (and its neighbourhood) a value of the parameter which makes it possible to count it among those belonging to the edge or not. Variance of the grey levels in the point's neighbourhood is the parameter deciding a bout counting it as belonging to the edge.

The second stage consists in using the averaging filtration selectively to those areas, which were selected for that on the first filtration stage. Points counted as belonging to the edge remain intact, therefore, blurring the edges is avoided. The next stage during defining the image parameters is calculating the pixels intensity values along the profile lines in the image. Points distributed evenly along the specified path and their intensity is determined by means of interpolation in the grey scale for each point. The MLP type (multilayer perceptron) unidirectional neural

networks were used to carry out correct classification of the analysed image into the particular life exhaustion classes. Images of structures divided into four classes according to the classification schema shown in Figure 16 are used for network training. Structure images prepared in the analogous way and not used in the training procedure will be used for verification. The obtained parameters of the structure image are entered to the network input, on its output, however, there is only a single neuron determining the material's life exhaustion extent.

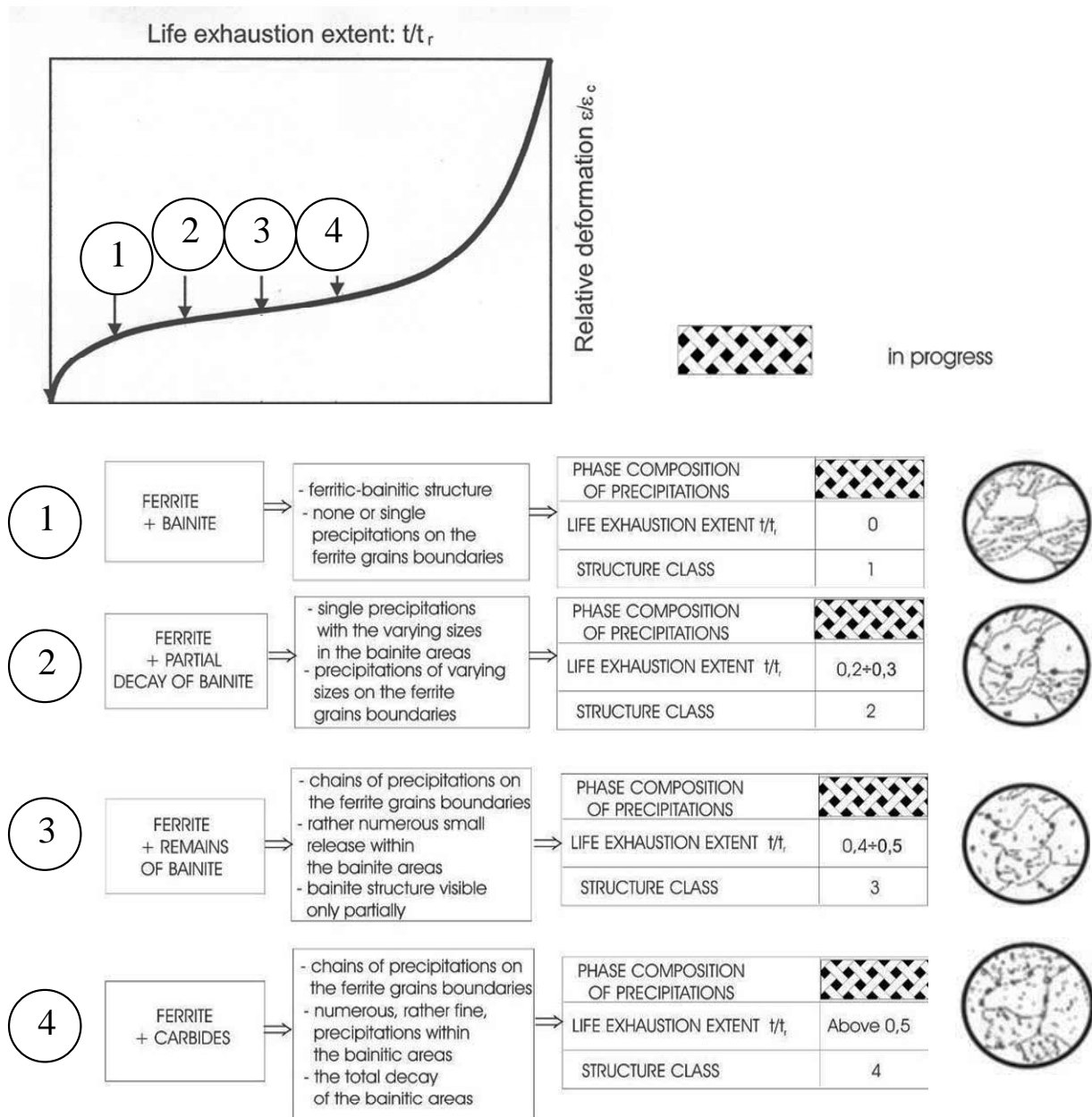


Fig. 16. Schema of structure changes during the long-time creep service of the low-alloy Cr-Mo steel type with micro-additions with the ferritic-bainitic structure in the initial state

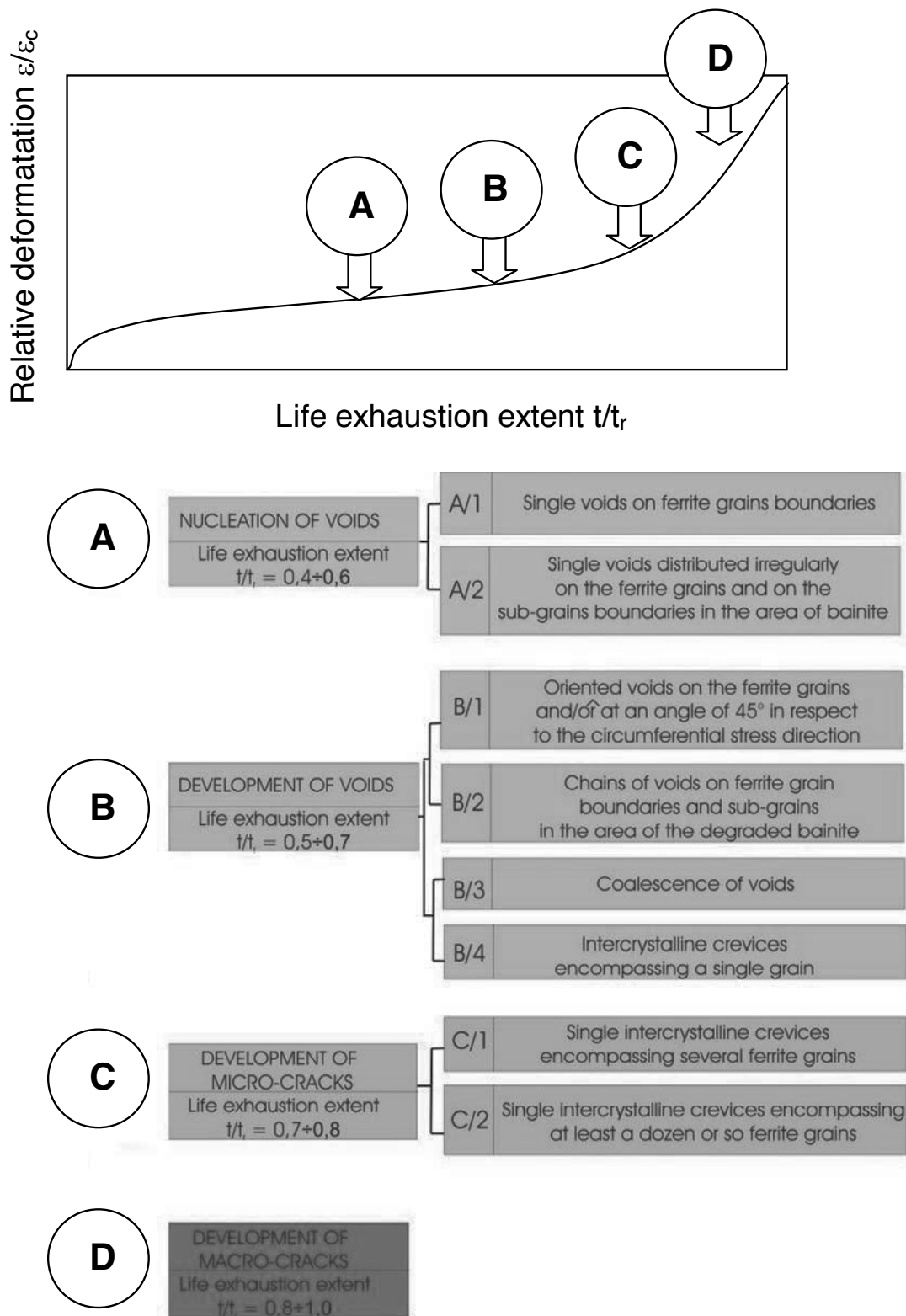


Fig. 17. Development of the internal damages after creep, depending on the life exhaustion extent  $t/t_r$ , and the relative strain  $\varepsilon/\varepsilon_c$  for the low-alloy Cr - Mo steel type with the ferritic-bainitic structure

## 4. Discussion of the investigation results

The long time annealing up to 3000 hours carried out for the T23 steel at the temperature close to the service temperature (550 and 600°C) did not cause the significant degradation of the KCV impact strength neither of the HV10 hardness. The impact strength is high and is about 250 J/cm<sup>2</sup>, and the hardness relevant to this state is from 190 to 220 HV10 (Figure 2). Also the structure after 3000 hours of annealing time did not undergo any significant changes and it is the ferrite with bainite and precipitations along the ferrite grain boundaries and sub-grains in the area of bainite (Figure 4).

Fractures of the impact strength test pieces after 3000 hours annealing time are mixed fractures; however, with a significant predominance of the ductile areas over the areas with the cleavage planes characteristic of the brittle fractures (Figure 5).

Observations of the T23 structure changes resulting from the simultaneous effect of temperature and stress, i.e., due to creep, revealed at magnification of up to 1000x only some slight changes in regards to the initial state structure. These changes are demonstrated by the slight increase of the amount of precipitations along the ferrite grain boundaries and sub-grains boundaries in the area of bainite as well as by appearance of rather numerous precipitations in the ferrite grains and bainite areas (Figure 6). However, observations carried out at bigger magnifications, i.e. 2000-3000x revealed a partial decay of the bainite areas, appearance of the precipitation chains on the ferrite grain boundaries and boundaries of sub-grains in the areas of bainite, and within the ferrite grains originated after the bainite sub-grains decay (Figure 7). Examinations of the microstructure and development of the precipitation processes after long time annealing and after creep tests to break were carried out on thin foils on the transmission electron microscope [4].

The microstructure matrix observed in the material after annealing at the temperature of 550°C for 1000 hours is made of the polygonized bainite with the partially retained lath structure (Figure 10). Precipitations of the M<sub>23</sub>C<sub>6</sub> carbides occur mostly at the ferrite grain boundaries (Figure 10a) and sub-grains in the areas of bainite (Figure 10b). Precipitations inside of the ferrite grains (Figure 10c) may be qualified as the M<sub>7</sub>C<sub>3</sub> carbides basing on their morphological features. The polygonized bainite with ferrite feature the material matrix after 3000 hours of annealing at this temperature. Precipitations occurring along the ferrite grains boundaries are probably the M<sub>23</sub>C<sub>6</sub> carbides (Figure 11a). The morphological features of precipitations observed inside the ferrite grains may suggest that they are the MX type carbides (Figure 11b).

The long term annealing at the temperature of 600°C for 1000 hours revealed the structure with the matrix in which the polygonized bainite with the clearly marked sub-grains prevails (Figure 12a). The significantly smaller dislocation density was observed in the ferrite grains (Figure 12b) than in the bainite areas. Rather big M<sub>23</sub>C<sub>6</sub> carbides occur both at the grain boundaries of the former austenite (Figure 12a) and at the ferrite grains boundaries (Figure 12b). The polygonized bainite with the clearly defined sub-grains (Figure 13a) also dominates in the

matrix structure after 3000 hours of annealing the material at this temperature. Rather big M<sub>23</sub>C<sub>6</sub> carbides occur in the chain form, mostly along the grain boundaries (Figure 13a,b).

Microstructure of the T23 steel after creep test to break with the test period of 10000 hours is a strongly polygonized bainite, yet with the small dislocation density (Figure 14a). Boundaries of ferrite grains and of sub-grains in the areas of the polygonized bainite are tightly packed with the M<sub>23</sub>C<sub>6</sub> carbide forming chains (Figure 14b).

Recapitulating, one may state that both the long term annealing at the temperature a close to the service one, as well as creep are the causes of the significant changes in the structure. These changes are demonstrated first with the partial, and next with total decay of the bainitic areas. The decay of the bainitic areas is accompanied by development of the precipitation processes. The long term temperature action causes increase of the amount of precipitations, their coagulation, coalescence, and growth. Precipitations appear both at the ferrite grain boundaries and also on boundaries of sub-grains in the bainite areas.

The simultaneous action of temperature and stress intensifies development of the precipitation processes, promoting them at the same time. Only the ferrite grains with the chains of precipitations along the grain boundaries, and numerous precipitations inside grains, are left in the structure after the long time joint action of temperature and stress. This causes deterioration of the creep resistance of the material in comparison with its state before service. This structure may be prone to generating internal defects resulting from further action of the temperature-stress parameters. First, defects in the form of the single voids will appear, and next in the form of the oriented voids and chains of voids. The surface transcrystalline crevices form resulting from the coalescence, encompassing initially a single, and then several and a dozen or more grains. This causes forming of the micro- and next macro-cracks, leading to the total cohesion loss of the material. Examples of some successive stages of the development of the internal defects in the T23 steel with the ferritic-bainitic structure are shown in Figure 15 [4].

Basing on observation of changes occurring in the material in creep the schema of these changes was proposed along with its successive stages, depending on the life exhaustion extent  $t/t_r$ , assigning the structure classes to them. Schema of such changes is shown in Figure 16. In Figure 17, however, classification of the internal defects development is shown, depending on the life exhaustion extent  $t/t_r$ , assigning the structure classes to the successive stages of their development [4].

Method for automatic classification of the extent of life exhaustion extent for the investigated steel is based on schema presented in Figure 16. Investigation results demonstrate that neural networks are a very useful classification tool. The values of the neural network quality coefficients for the optimum neural network model prove the correct representation of the modelled classification and the generalisation ability of the developed neural network.

The presented method for classification of structure changes and development of the internal damages will be verified and developed further as the existing characteristics and database content for the investigated steel will be extended.

## 5. Conclusions

The presented investigation results are the effect of completing the first stage of investigation of changes of properties and structure resulting from the simultaneous action of temperature and stress on the material. Result of investigation are convergence with result obtained in another scientific laboratories [2, 10, 13-15]. The developed classification of structure changes, of the precipitation processes development, and processes of the internal defects, as well as the life exhaustion extent assigned to them will make assessment of the T23 steel state possible, as well as it will make it possible to determine its usefulness for the further safe service at the working service parameters.

The developed method for automatic classification and assessment of the material state basing on its structure image will be an element assisting the material diagnostics system for the investigated steel.

## References

- [1] A. Bensaoula, H.A. Malki, A.M. Kwari, The Use of Multilayer Neural Networks in Material Synthesis, IEEE Transactions on Semiconductor Manufacturing 11 (1998) 421-431.
- [2] F. Deshayes, W. Bendick, K. Haarmann, J.C. Vaillant, New 2-3%Cr Steel Grades for Waterwall Panels and Superheaters, Report COST 501 –Liege, 1998.
- [3] J. Dobrzański, Development of the service characteristics of the new generation steel for design of the pressure elements of the supercritical pressure boilers - working out of data for designers, manufacturers, and users of power industry equipment, Report from the research project No. PZ-00003/9/BM/2002 - unpublished (in Polish).
- [4] J. Dobrzański, A. Zieliński, Characteristics of changes of structure and properties occurring in service of the new generation steel (2.5-12%Cr) for pressure elements of the supercritical pressure boilers, Project Report IMŻ No. S0-0438/BE/03 – unpublished (in Polish).
- [5] J. Dobrzański, A. Zieliński, M. Sroka, Structure, properties and method of the state evaluation of low-alloyed steel T23 (HCM2S) worked in creep conditions, Proceedings of the 11<sup>th</sup> International Scientific Conference “Contemporary Achievements in Mechanics, Manufacturing and Materials Science” CAM3S’2005, Gliwice–Zakopane, 2005 (CD-ROM).
- [6] L.A. Dobrzański, J. Dobrzański, J. Madejski, J. Załona, The computer system for forecasting of the life of the pressure loaded power installation elements, Journal of Materials Processing Technology 48 (1995) 551-560.
- [7] L.A. Dobrzański, M. Krupiński, J.H. Sokołowski, Computer aided classification of flaws occurred during casting of aluminum, Journal of Materials Processing Technology 167 (2005) 456-462.
- [8] L.A. Dobrzański, M. Sroka, J. Dobrzański, Application of neural networks to classification of internal damages in steels working in creep service, Journal of Achievements in Materials and Manufacturing Engineering 20 (2007) 303-306.
- [9] L.A. Dobrzański, M. Sroka, W. Sitek, M. Krupiński, J. Dobrzański, Computer aided for classification of damage of steel working in creep conditions, Metallurgist 3 (2005) 176-182 (in Polish).
- [10] J. Hakl, T. Vlasak, P. Brziak, P. Zifcak, Contribution to the investigation of advanced low-alloy P23 steel creep behavior, Proceedings of the International Scientific Conference “Materials for Advanced Power Engineering”, Liege, 2006, 985-996.
- [11] Q. Hancheng, X. Bocai, L. Shangzheng, W. Fagen, Fuzzy neural network modeling of material properties, Journal of Materials Processing Technology 122 (2002) 196-200.
- [12] C.Z. Huang, L. Zhang, L. He, J. Sun, B. Fang, B. Zou, Z.Q. Li, X. Ai, A study on the prediction of the mechanical properties of a ceramic tool based on an artificial neural net, Journal of Materials Processing Technology 129 (2002) 399-402.
- [13] N. Komai, T. Imazato, Effect of tempering times on creep strength in ASME Gr.23(2.25Cr-1.6W steel), Proceedings of the International Scientific Conference “Materials for Advanced Power Engineering”, Liege, 2006, 997-1009.
- [14] M.E. Staubli, Final summary report of turbine groupe. COST 522 – steam power plant, Baden, 2003.
- [15] M.E. Staubli, K.H. Mayer, T.V. Kern, R.W. Vanstone, The European Collaboration in advanced steam turbine materials for ultra efficient, low emission power plants, Proceedings of the International Scientific Conference “Advanced Materials for 21st Century Turbines and Power Plants” PARSON 2000, London, 2000, 98-107.
- [16] Y.J. Xing, J. Xing, J.,Sun, L. Hu, An improved neural networks for stereo-camera calibration, Journal of Achievements in Materials and Manufacturing Engineering 20 (2007) 315-318.
- [17] J. Trzaska, L.A. Dobrzański, Application of neural networks for selection of steel with the assumed hardness after cooling from the austenitising temperature, Journal of Achievements in Materials and Manufacturing Engineering 16 (2006) 145-150.
- [18] ASME Case 2199 – cases of ASME Boiler and Pressure Vessel Code – Seamless 2,25Cr-1,6W-V-Nb, Materials Section, 1, 1995.
- [19] ASTM A213/A213M-99A – Standard Specification for Seamless Ferritic and Austenitic Alloy – Steel Boiler, Superheater, and Heat-Exchanger Tubes.
- [20] Materials from SUMITOMO Metal Industries Ltd No 903F-2666, 906F-3220, 908F-3403 Development of High Strength 2,25Cr-1,6W-V-Nb Steel Tube (HCM2S) for Boiler Application, 1993, 1998.